



Structural, Electronic, Magnetic, and Optical Properties of Sm Doped ZnS: A First Principle Study

Hareem Mufti^{1*}, Fatima Manzoor¹, Nisar Ahmad², Surraya Mukhtar¹, Mujahid Niaz Akhtar³, Ghauri Sabir⁴

¹ Department of Physics, Allama Iqbal Open University, Islamabad, Pakistan

² Department of Physics and Applied Mathematics (DPAM), Pakistan Institute of Engineering and Applied Sciences (PIEAS), Nilore, Islamabad

³ Govt. Alamdar Hussain Isamia Graduate College, Multan, Pakistan

⁴ School of Electrical and Computer Engineering, Faculty of Computing, Engineering and Mathematical Sciences, Frenchay Campus, University of the West of England Coldharbour Lane, Bristol BS 161Qy, London, UK

ARTICLE INFO

ABSTRACT

Article History:

Received: August 14, 2023
Revised: October 18, 2023
Accepted: December 29, 2023
Available Online: December 30, 2023

Keywords:

Zinc Sulfide
Density Functional Theory
Samarium
Magnetic Properties
Optical Properties

Wide band gap semiconductors have many applications in photo luminescence devices and optoelectronic devices. We have investigated the structural, magnetic and optical properties of pure ZnS and Sm doped ZnS using density functional theory and implemented first principle linearized augmented plane wave (LAPW) method. For exchange correlation potential energy, generalized gradient approximation (GGA), GGA+U (where U is Hubbard potential) and Tran and Blaha modified Becke-Johnson (TB-mBJ) approximations are used. ZnS is a wide band gap semiconductor material having experimental band gap ~ 3.54 eV. In this study band gap of pure ZnS was calculated as 1.963 eV, 2.124 eV and 3.574 eV by using GGA, GGA+U and TB-mBJ approximations. GGA+U approximation was used for spin polarized calculations of ZnS: Sm shows ferromagnetic (FM) behavior of doped semiconductor with band gap is 2.75eV. Pure ZnS is isotropic material while after doping with Sm it becomes anisotropic material. Ultraviolet and visible radiations are absorbed in these materials hence they can have potential applications in optoelectronic devices.

OPEN ACCESS

© 2023 The Authors, Published by iRASD. This is an Open Access article under the Creative Common Attribution Non-Commercial 4.0

*Corresponding Authors' Email: hareem.mufti@aiou.edu.pk

1. Introduction

The most popular and widely used computational technique for simulating various materials in solid-state physics, chemistry, material physics, chemical engineering, geology, and other fields is density functional theory (David Sholl, 2009). Zinc Sulfide is a compound semiconductor material with a large and straight band gap. Due to their potential usage in devices at high temperatures and strong electric fields, they are of great technological interest (Singh, 2005). ZnS has a direct band gap semiconductor of 3.54eV (O. Madelung, 1982). ZnS are in two crystalline structures that are cubic and hexagonal. We used cubic structure in this research work, in which optical properties are isotropic and x, y and z axes are identical (Fox, 2010). ZnS has a applications in electroluminescent devices, solar cell and optoelectronic devices (S.Q. Wang, 2006). Moreover, ZnS is credited to be one of the top likely materials for blue-light diodes (Fatma Göde, 2007) and electro-luminescent displays (Hasse MA, 1991; Poulomi Roy, 2006). Mostly physical properties is understood from the study of electronic band structure of materials (I. A. Imad Khan, 2013).

The structural, magnetic, electronic and optical properties of ZnS are studied experimentally and theoretically but in Sm: ZnS no information is on the subject is available in the literature.

Properties of pure ZnS and Sm doped ZnS are calculated by using GGA, GGA+U and TB-mBJ but TB-mBJ is considered as the good approach of II-VI semiconductors for the calculations of band gap (I. A. Imad Khan, 2013; I. A. a. D. Z. Imad Khan, 2013; Imad Khan, 2012; I. A. a. H. A. R. A. Imad Khan, 2013; Imad Khana, 2012).

The detailed computational methodology is described in next section. Results and discussion are outlined in section 3 and conclusion described in section 4.

2. Computational Method

The structural, magnetic, electronic and optical properties are investigated by using the GGA, GGA+U and TB-mBJ to find out the exchange potential as implemented in the WIEN2K package (Blaha P, 2001). In GGA+U value of 6.0 eV for $U_{eff} = U - J$ is used as described for lanthanides in reference (E. V. D. van Loef, 2001).

In these calculations RMT was selected in that way in which total energy is converged and no charge leakage from the core.

The plane wave cut-off value of $K_{max}=10/RMT$ was used for the wave function in the interstitial area. A fine k mesh of 1000 was employed in the Brillouin zone integration, and convergence was assessed using self-consistency.

The configurations of valence atomic electron of Zn, S and Sm are $3d^{10}4s^2$, $3s^23p^4$ and $4f^66s^2$ respectively. A complicated dielectric function can be used to express a material's linear response to electromagnetic radiation.

$$\varepsilon(\omega) = \varepsilon_1(\omega) + i\varepsilon_2(\omega) \quad (1)$$

Self-consistent electronic structure computations have been used to determine the absorptive (imaginary) component of $\varepsilon(\omega)$ (Wang, 1992). The formula for $\varepsilon_2(\omega)$ is as follows (AmineSlassi, 2015):

$$\varepsilon_2(\omega) = \frac{8}{2\pi\omega^2} \sum |P_n(k)|^2 \frac{dS_k}{\Delta\omega_n(k)} \quad (2)$$

$P_n(k)$ is the dipole momentum of the outer band transition. $\varepsilon_2(\omega)$ is the imaginary dielectric function describes the transition momentum matrix element and DOS. $\varepsilon_1(\omega)$ is the real dielectric function obtained from $\varepsilon_2(\omega)$ from Kramers kronig relation that is shown below (AmineSlassi, 2015).

$$\varepsilon_1(\omega) = \frac{2}{\pi} P \int_0^\infty \frac{\omega' \varepsilon_2(\omega')}{\omega'^2 - \omega^2} d\omega' \quad (3)$$

3. Results and Discussions

3.1. Structural Properties

Zinc Sulfide (ZnS) exists in two crystalline forms, cubic and hexagonal. In this research work cubic crystal structure is used. Zinc blende unit cell is shown in figure 1. Figure 1 shows that Zn atom is at origin and S atom is at $\frac{1}{4}$ positions. In zinc blende structure, angle is $\alpha=\beta=\gamma=90$ and lattice type is F-43.

We optimized every unit cell to examine the structural properties of ZB. After volume optimization stable ground state energy is gained. Murnaghan's equation uses the optimal values to determine the structural parameters, such as lattice constants (Birch, 1947). Table 1 presents a comparison between the estimated lattice parameters for ZnS using the GGA approach and the known experimental results.

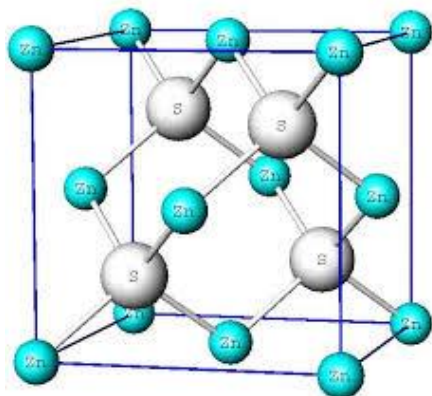


Figure 1: Crystal structures of zinc-blende (ZnS)

Table 1

Calculated lattice constants for pure ZnS by using GGA and compared with experimental and other theoretical results

ZnS	Lattice parameter (Å)
Experimental	5.412 (S. Ves, 1990)
Other theoretical	5.342 (Rabah khenata, 2006)
Optimized (GGA)	5.446 (Jian-Ping Tang, 2013)
	5.457

The outcomes demonstrate that a lattice constant is predicted by the GGA computations of 5.457 Å, which is approximately equal to other theoretical calculations but overestimates (0.04%) the experimental value.

We have discovered through structural optimization studies that the addition of Sm impurities results in the ZnS crystal lattice expanding. To investigate how impurities affect ZnS's optical and structural characteristics, we used 1x1x2 super cells. In super cell total number of atoms is 16 in which 8 atoms of Zinc and 8 atoms of sulfur. In super cell 2 atoms of Zn is replaced by Sm hence it is 25% doping in pure crystal.

3.2. Electronic Properties

Band gap of pure and doped ZnS is estimated by using different approximations like GGA, GGA+U and TB-mBJ from the calculations of electronic structure. We know that GGA is not good technique for the calculations of the calculations of energy gaps in insulators and semiconductors. GGA+U and TB-mBJ provide good results.

Calculations of electronic states of lanthanides compound (Sm: ZnS) by using GGA+U with $U_{eff} = 6.0\text{eV}$ gives a good agreement with experiment results.

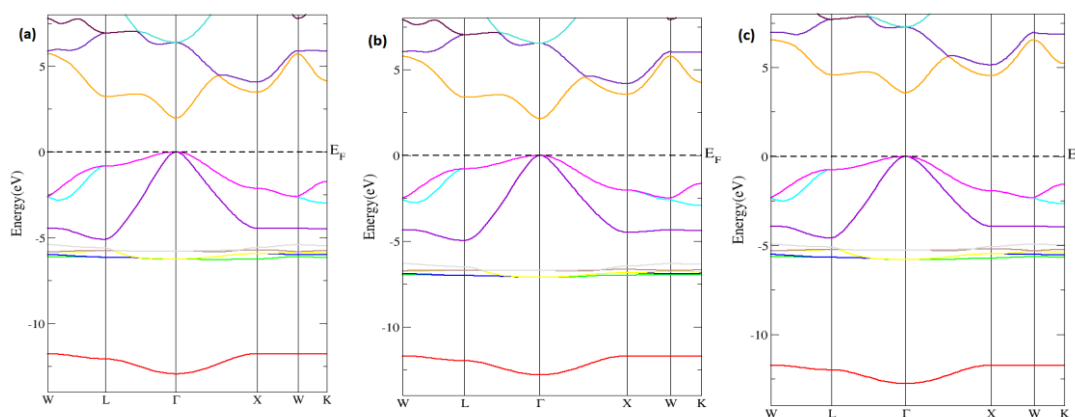


Figure 2: The calculated electronic band structure of pure ZnS by using (a) GGA (b) GGA+U (c) TB-mBJ

Electronic band structure of pure ZnS by using GGA, GGA+U and TB-mBJ approximations shows that in these three structures conduction band minimum (CBM) and valence band maximum (VBM) lie at a same K points, which shows that these are direct band gap material. Conduction band is dominated due to the Zn (4s) and S (3p) states. Valence band is due to Zn (3d) and S (3p) states and Zn-4s and S-3p hybridization. When compared to the experimental result displayed in Table 2, the calculated band gap is about equal when using the TB-mBJ approach and underestimated when using the GGA and GGA+U methods..

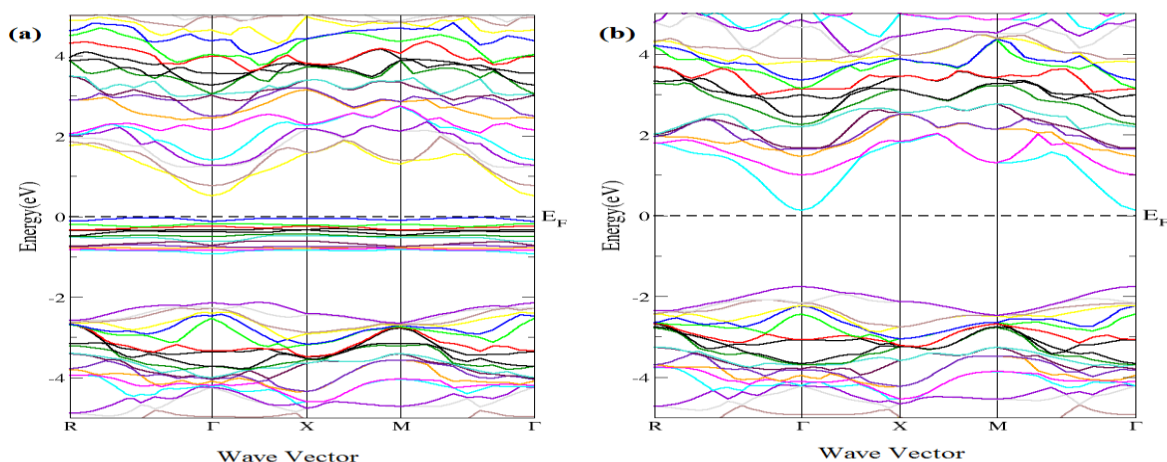


Figure 3: Calculated electronic band structure of Sm doped ZnS for FM calculations by using GGA+U (a) majority spin (b) minority spin

Figure 3 shows the band structure of Sm doped ZnS for FM calculations by using GGA+U figure (a) shows the band structure of spin up states or majority spin electrons and figure (b) shows the band structure of spin down states or minority spin electrons. 2.751 eV is the band gap of Sm doped ZnS.

After doping of Sm many states are occupied in band structure these are due to Sm 4f-states so that there are such narrow bands in the Conduction band and Valence band. As shown in figure (a) majority spin of Sm doped ZnS in which some states which are due to Sm-4f states lie near the Fermi level. Hence band gap is reduced after doping of Sm. Total and partial density of states (PDOS) of ZnS and Sm doped ZnS are computed for a more thorough examination of the electronic band structure; the findings are displayed in figure 4, 5 and 6.

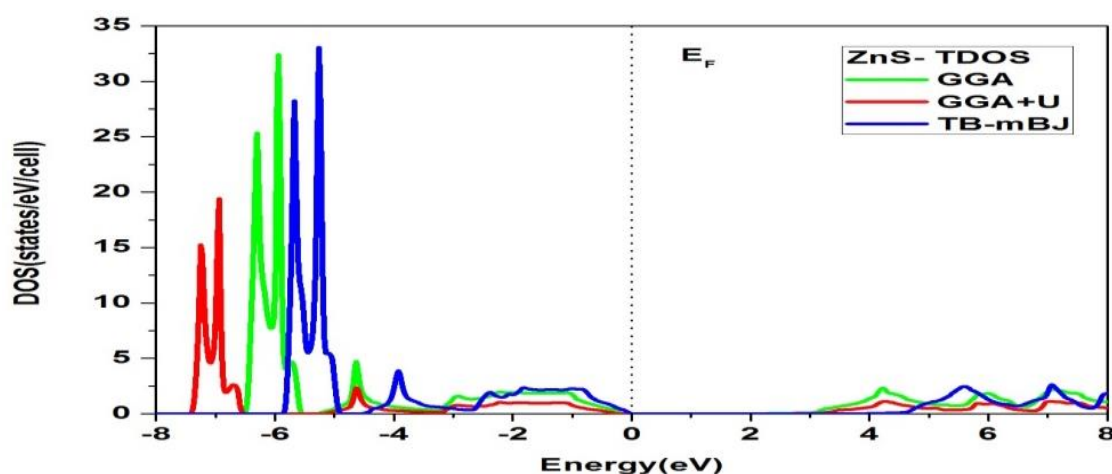


Figure 4: The calculated total density of states of ZnS by using GGA, GGA+U and TB-mBJ

Density of states investigated by using generalized gradient approximation (GGA), GGA+U (where U is Hubbard potential) and Tran and Blaha modified Becke-Johnson (TB-

mBJ) approximations as shown in figure 4. We compared the results from these approximations and found the correct approximation for our compound.

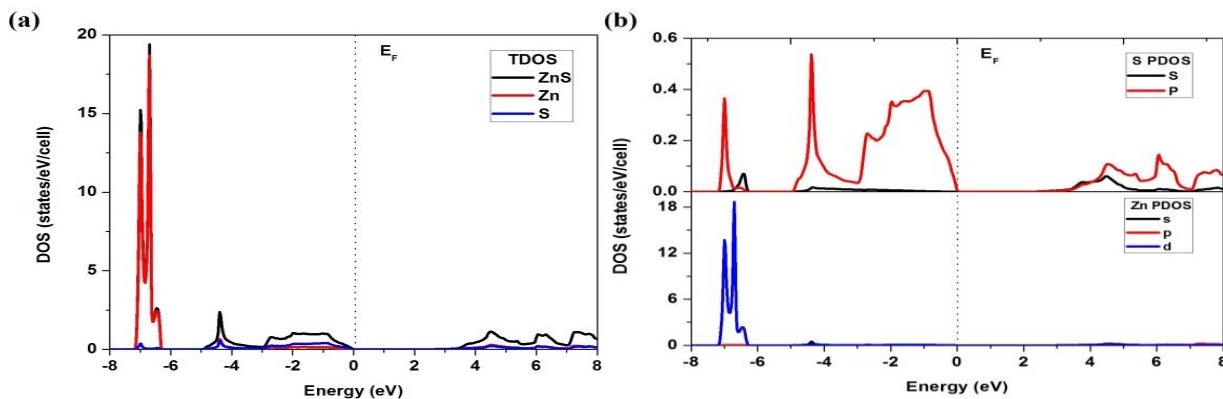


Figure 5: The calculated (a) TDOS of ZnS, Zn and s (b) PDOS of Zn and S states

The band gap between ZnS's valence and conduction bands is evident from the total DOS result in Figure. Three zones can be distinguished in the valence band density of states for the zinc-blende structure of zinc sulfide (ZnS). S atom 3p-states dominate the region between -6eV and -4eV, with Zn 4s-states contributing. Zn 3d-states predominate in the range between -8 eV and -6 eV, with a minor contribution from sulphur 3s and 3p-states. -3 to -1 state are due to contribution of 3p states of S. We investigated the ground level energy through ferromagnetic calculations of Sm doped ZnS.

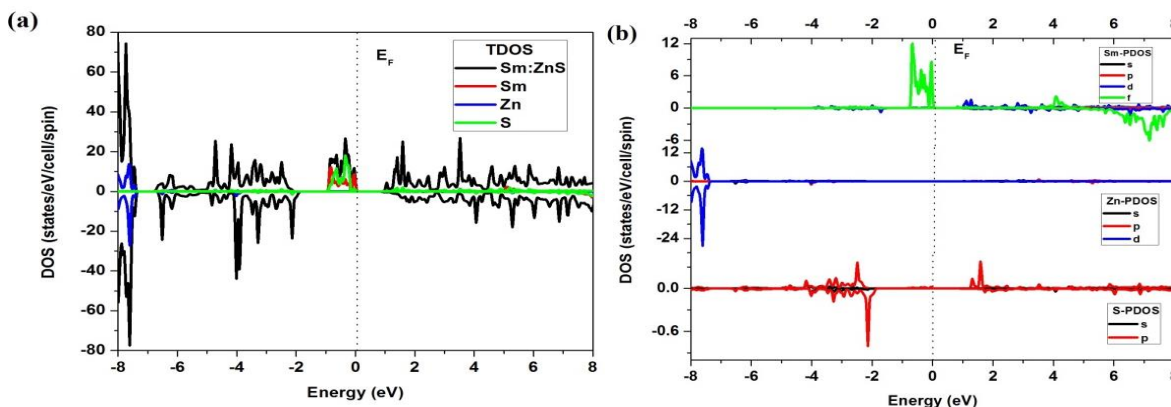


Figure 6: The calculated (a) TDOS of Sm, Zn and S (b) PDOS of Sm, Zn and S states

Figure 6(b) shows the partial density of states of Sm, Zn and S for their s, p, d and f states. From -9 to -7 eV states are due to Zn 3d states and from -4 to -2 due to Sulphur atom 3p states. States near the Fermi level that is from -1 to 0 is due to Sm 4f states. ZnS is compound semiconductor material after doping of Sm it becomes p-type semiconductor because valence band is very close to Fermi level which means holes can easily produce in this compound.

Table 2
Experimental and calculated band gap of pure and Sm doped ZnS by using different methods

Compound	Method	E _g (eV)
ZnS	Experimental	3.54 (Bredal M, 1998)
	Other theoretical	2.2 (Shimono, 2003)
	GGA	1.96
	GGA+U	2.12
	TB-mBJ	3.57
Sm:ZnS	GGA+U(FM)	2.75

3.3. Magnetic Properties

Magnetic properties of pure and doped ZnS are presented in this section. The ferromagnetic stability is calculated from Energy difference between the antiferromagnetic and ferromagnetic configuration from equation that is

$$\Delta E = E_{AFM} - E_{FM} \quad (4)$$

If difference is positive system is ferromagnetic. The total energy differences between the FM and AFM configuration shows that Sm: ZnS is ferromagnetic material at ground energy level.

Table 3

The calculated of FM and AFM ordering and static dielectric constant ($\epsilon_1^{\parallel}(0)$ and $\epsilon_1^{\perp}(0)$)

Compound	Sm:ZnS
$\Delta E(\text{eV})$	0.01
$\epsilon_1^{\parallel}(0)$	6.40
$\epsilon_1^{\perp}(0)$	6.37

Pure ZnS is non-magnetic material after doping of Sm it becomes magnetic material.

3.4. Optical Properties

ZnS has a direct and wide band gap material and is of great importance in photonic devices and optical communication applications.

Some of the electronic band processes that contribute to the optical properties of solids are optical conductivity, electron energy loss function, absorption coefficient, reflectivity, and epsilon. The material's optical characteristics are described by the dielectric function. The optical parameters of pure ZnS such as refractive index (n), absorption coefficient $I(\omega)$, electron energy loss function $L(\omega)$, optical conductivity $\sigma(\omega)$, reflectivity $R(\omega)$, extinction coefficient (k) and dielectric function $\epsilon(\omega)$ are calculated.

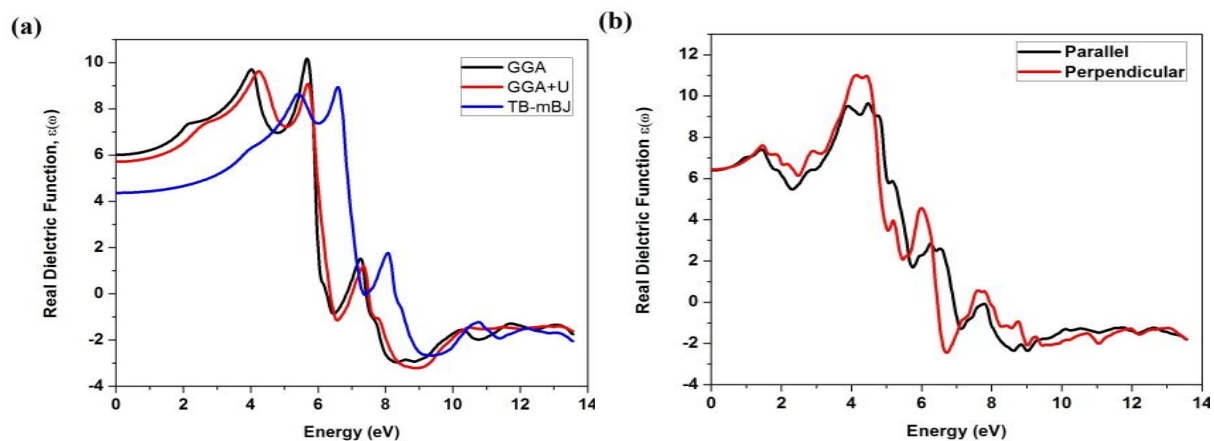


Figure 7: The calculated real Dielectric Function $\epsilon(\omega)$ of (a) pure ZnS by using GGA, GGA+U and TB-mBJ (b) Sm doped ZnS by using GGA+U parallel and perpendicular component

Pure ZnS is isotropic material in which parallel and perpendicular component lie at a same line figure 7(a) shows parallel and perpendicular component lie at a single line, three lines shows a real dielectric function from GGA, GGA+U and TB-mBJ. After doping of Sm it becomes anisotropic material.

Table 4
The static real dielectric constant $\epsilon(0)$ by using GGA, GGA+U and TB-mBJ approximations

Compound	ZnS
$\epsilon(0)$	6.01 (GGA)
	5.71 (GGA+U)
	4.37 (TB-mBJ)

Static dielectric constant is very essential term in real part of dielectric function. The numerical value of static real dielectric constant $\epsilon(0)$ of pure ZnS without any contribution from lattice vibration is shown in table 4. Figure (b) represents real part of dielectric function of Sm: ZnS, in which parallel and perpendicular components are shown, its numerical value of parallel and perpendicular component are presented in table 3. In Sm doped ZnS the value of $\epsilon_1^{\parallel}(0)$ is greater than $\epsilon_1^{\perp}(0)$ which shows that these materials are more transparent to parallel direction (\parallel) than perpendicular (\perp) direction.

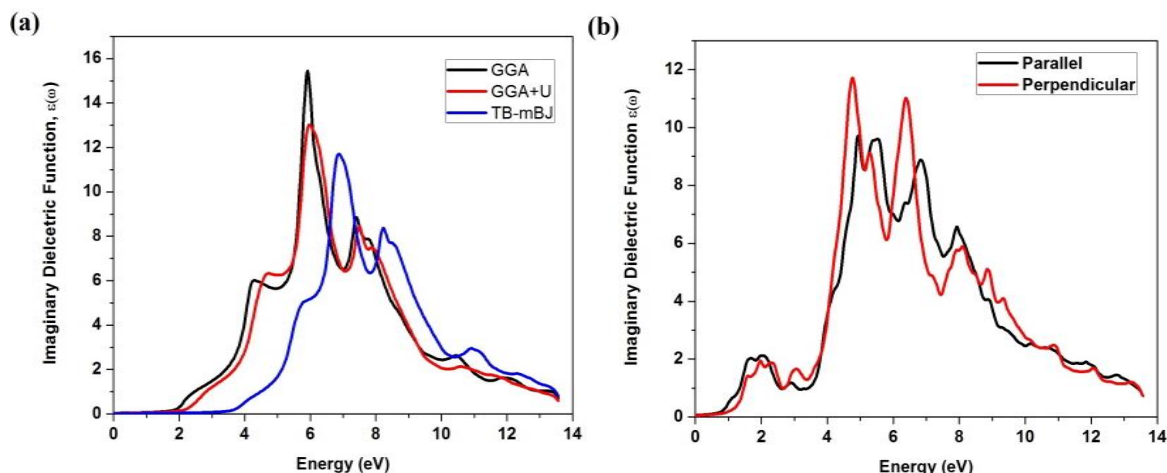


Figure 8: The calculated imaginary dielectric function $\epsilon(\omega)$ of (a) pure ZnS by using GGA, GGA+U and TB-mBJ (b) Sm doped ZnS by using GGA+U parallel and perpendicular component

Figure (a) shows that imaginary dielectric function by using GGA, GGA+U and TB-mBJ in which highest peaks situated at 5.88, 5.95 and 6.84 eV respectively. In figure (b) parallel and perpendicular component of Sm doped ZnS is shown. From figure (b) we know that magnitude of ϵ_2^{\perp} is greater than ϵ_2^{\parallel} which shows that anisotropy in perpendicular direction is greater than parallel direction.

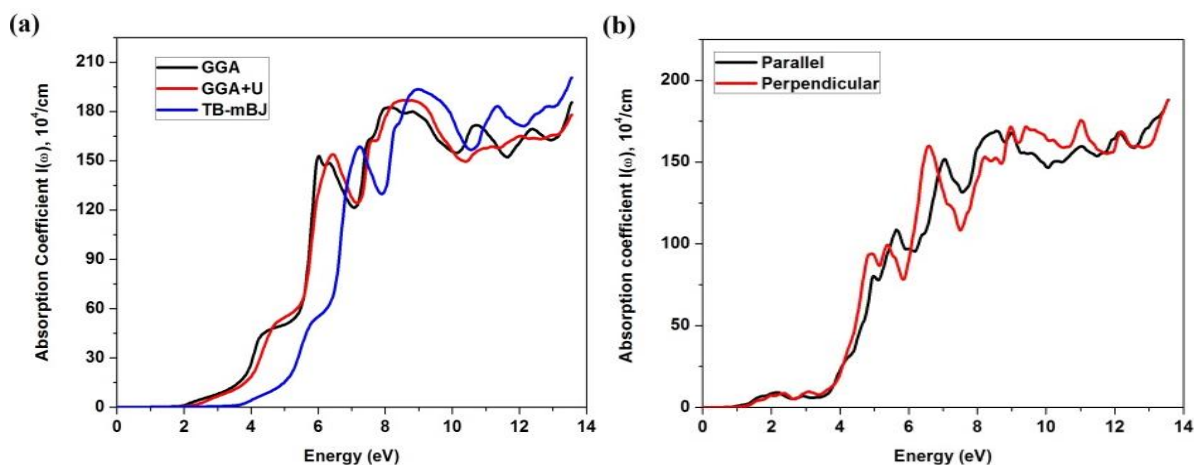


Figure 9: The calculated absorption coefficient $I(\omega)$ (a) pure ZnS by using GGA, GGA+U and TB-mBJ (b) Parallel and perpendicular component of Sm doped ZnS by using GGA+U

In figure 9(a) the plot of absorption coefficient spectrum $I(\omega)$, has its maximum arises at 6.00eV (206.64nm), 6.33eV (195.87nm) and 8.88eV (139.62nm) by using GGA, GGA+U and TB-mBJ. In figure (b) $I(\omega)$ has its maximum arises of parallel component is at 7.03eV (176.36nm) and perpendicular component is at 6.57eV (218.67nm) from GGA+U. From these graphs it is clear that maximum reflectivity occurs at ultraviolet region ($\lambda=400-10\text{nm}$).

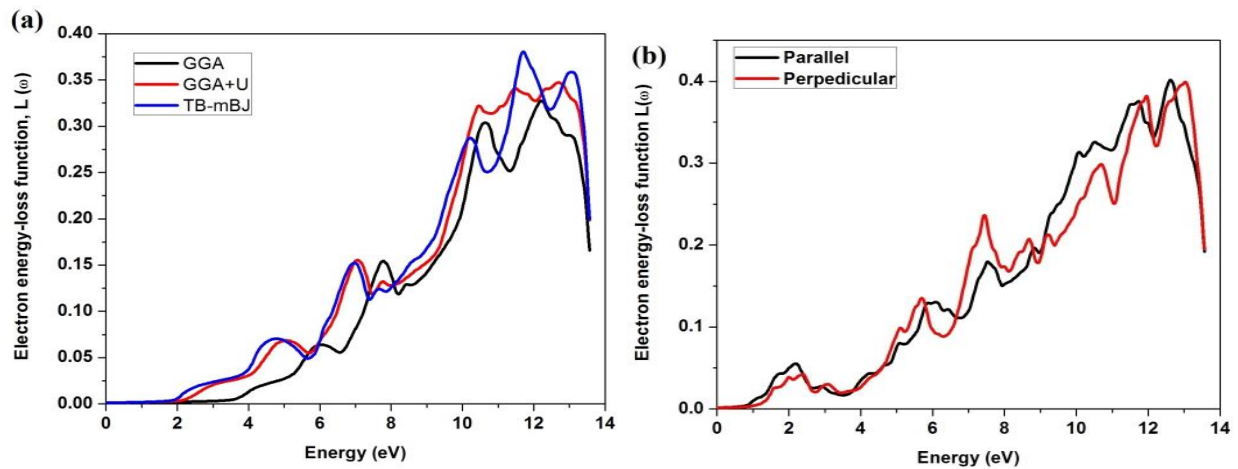


Figure 10: The calculated Electron energy-loss function of $L(\omega)$ of (a) pure ZnS by using GGA, GGA+U and TB-mBJ (b) parallel and perpendicular component of Sm doped ZnS by using GGA+U

$L(\omega)$ is the electron energy loss function that is a meaningful factor unfolding the energy loss of a fast moving electron passing through a material. Figure 10 (a) shows that $L(\omega)$ increasing gradually at the energy of 2eV and increases continuously till 12 eV with sharp and broad peaks by using GGA, GGA+U and TB-mBJ. Figure 10(b) shows that $L(\omega)$ increases at the energy of 1eV and increasing continuously at 13 eV with sharp and broad peaks by using GGA+U.

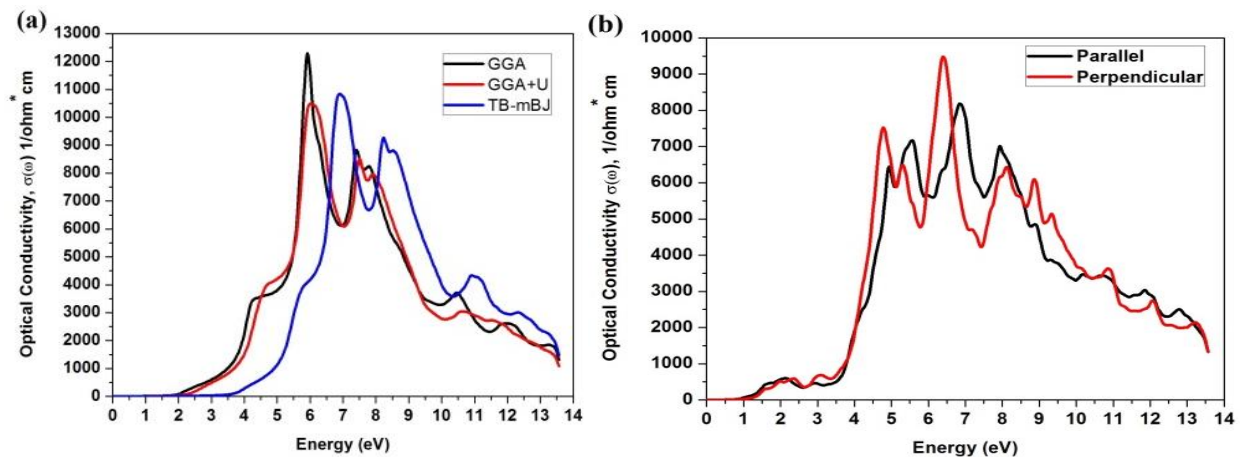


Figure 11: The calculated optical Conductivity $\sigma(\omega)$ of (a) pure ZnS by using GGA, GGA+U and TB-mBJ (b) parallel and perpendicular component of Sm doped ZnS by using GGA+U

The maximum optical conductivity $\sigma(\omega)$ was noticed at 5.89, 5.99 and 6.89eV by using GGA, GGA+U and TB-mBJ respectively. Figure 11(b) shows parallel and perpendicular component maximum optical conductivity $\sigma(\omega)$ is at 6.87 and 6.408eV respectively.

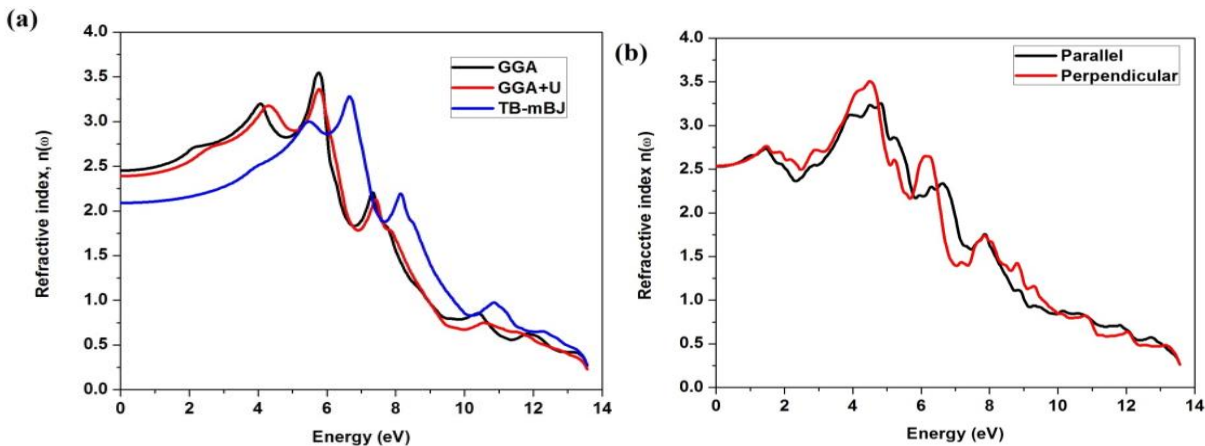


Figure 12: The calculated Refractive index $n(\omega)$ of (a) pure ZnS by using GGA, GGA+U and TB-mBJ (b) parallel and perpendicular component of Sm doped ZnS by using GGA+U

The calculated static refractive index $n(0)$ of pure ZnS and Sm doped ZnS of parallel and perpendicular component is shown in figure 12 (a) and (b) and its numerical value are given in table 5.

Table 5
The calculated static refractive index ($n(0)$, $n^{\parallel}(0)$ and $n^{\perp}(0)$)

Compound	ZnS	Sm:ZnS
$n(0)$	2.45 (GGA) 2.39 (GGA+U) 2.09 (TB-mBJ)	----- ----- -----
$n^{\parallel}(0)$	-----	2.53 (GGA+U)
$n^{\perp}(0)$	-----	2.54 (GGA+U)

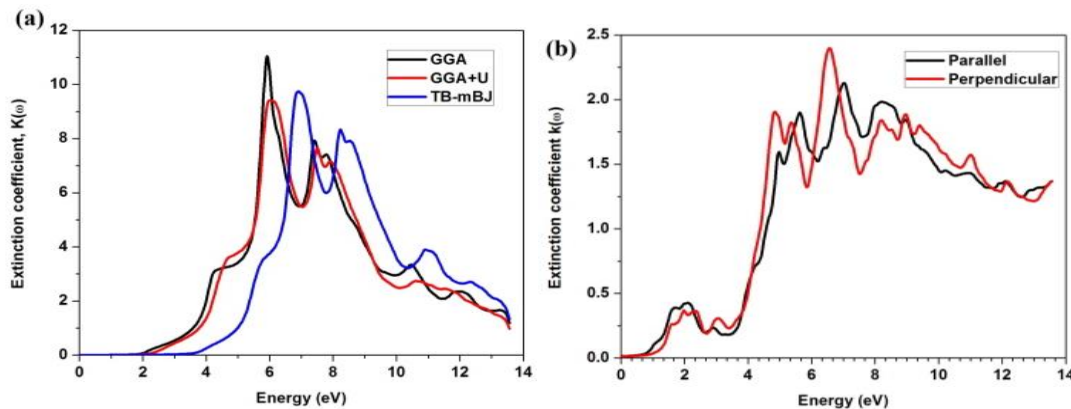


Figure 13: The calculated Extinction coefficient $K(\omega)$ (a) pure ZnS by using GGA, GGA+U and TB-mBJ (b) parallel and perpendicular component of Sm doped ZnS by using GGA+U

The calculated extinction coefficient $k(\omega)$ of pure ZnS has maximum values at 6.00, 6.27 and 7.14 eV by using GGA, GGA+U and TB-mBJ respectively, as shown in Figure 13(a). Extinction coefficient $k(\omega)$ of Sm doped ZnS of parallel and perpendicular component has maximum values at 7.04 and 6.58 eV by using GGA+U respectively, as shown in Figure 13(b).

4. Conclusion

Structural, magnetic and optical properties of pure and rare earth doped ZnS are calculated by using LO+LAPW method. GGA, GGA+U and TB-mBJ approximation are used for exchange correlation potential. Results show that lattice constant of ZnS by using GGA approximation is equal to other reported theoretical results and 0.04% overestimated from

experimental value. Band gap of pure ZnS was calculated as 1.96eV, 2.12eV and 3.57eV by using GGA, GGA+U and TB-mBJ approximations, respectively. TB-mBJ is found to be best among all the approximations used in this study for calculation of band gap of pure ZnS as estimated band gap is in close agreement to experimental value. Spin polarized calculations of Sm doped ZnS are investigated via GGA+U approach and results reveals that energy difference of Sm doped ZnS is 0.012 Ry, it is FM at ground energy level.

ZnS is isotropic material while doping of Sm it becomes anisotropic material. ZnS after doping of Sm becomes P type semiconductor material. Pure ZnS band gap calculated is 3.57eV and after doping of Sm band gap reduced to 2.75eV. Narrow band gap materials have many applications as detection and generation of infrared radiation, television coverage, used as infrared source, detector for the military, earth observation systems, process control system, environment monitoring system, infrared astronomy and commercial applications. Therefore this study will be helpful in further experimental research.

Reference

- AmineSlassi. (2015). Electronic structure and optical properties of Cu_3PX_4 (X=S and Se): Solar cell made of abundant materials. *Materials Science in Semiconductor Processing*, 39, 217-222.
- Birch, F. (1947). Finiteelastic strain of cubic crystals. *Phys Rev*, 71(11).
- Blaha P, S. K., Madsen G K H. (2001). *WIEN2K:an augmented plane wave plus local orbitals program for calculating crystal properties*. Vienna, Austria, : Vienna University of technology.
- Bredal M, M. J. (1998). ZnS precipitation: morphology control. *JOURNAL OF MATERIALS SCIENCE*, 33, 471 – 476.
- David Sholl, J. A. S. (2009). *Density Functional Theory: A Practical Introduction*.
- E. V. D. van Loef, P. D., and C. W. E. van Eijk. (2001). High-energy-resolution scintillator: Ce^{3+} activated LaBr_3 . *Applied Physics Letters*, 79(10), 1573.
- Fatma Göde, C. G., Muhsin Zor (2007). Investigations on the physical properties of the polycrystalline ZnS thin films deposited by the chemical bath deposition method. *Journal of Crystal Growth*, 299(1), 136-141.
- Fox, M. (2010). *Optical properties of solids* (second edition ed.): Oxford University Press, .
- Hasse MA, Q. J., DePuydt JM, Cheng H (1991). Blue-green laser diode. *Applied Physics Letters*, 59(11).
- Imad Khan, I. A. (2013). Theoretical studies of the band structure and optoelectronic properties of $\text{ZnO}_{1-x}\text{S}_x$ *International Journal of Quantum Chemistry*, 113(9), 1285-1292.
- Imad Khan, I. A. a. D. Z. (2013). Electronic and optical properties of mixed Be-chalcogenides. *Electronic and optical properties of mixed Be-chalcogenides*, 74(2).
- Imad Khan, I. A. a. H. A. R. A. (2012). Effects of phase transition on the optoelectronic properties of $\text{Zn}_{1-x}\text{Mg}_x\text{S}$. *Journal of Applied Physics*, 112(7).
- Imad Khan, I. A. a. H. A. R. A. (2013). Conversion of optically isotropic to anisotropic $\text{CdS}_x\text{Se}_{1-x}$ ($0 < x < 1$) alloy with S concentration. *Computational Materials Science*, 77, 145-152.
- Imad Khana, A. A., H.A. Rahnamaye Aliabad, Iftikhar Ahmada. (2012). Transition from optically inactive to active Mg-chalcogenides: a first principle study. *Computational Materials Science*, 61, 278-282.
- Jian-Ping Tang, L.-L. W., Wen-Zhi Xiao, and Xiao-Fei Li. (2013). First principles study on magnetic properties in ZnS doped with palladium. *The European Physical Journal B*, 86(362), 1-5.
- O. Madelung, L.-B. (1982). *Numerical Data and Functional Relationships in Science and Technology* (Vol. 17b). Berlin.
- Poulomi Roy, J. R. O., Suneel Kumar Srivastava. (2006). Crystalline ZnS thin films by chemical bath deposition method and its characterization. *Thin Solid Films*, 515(4).
- Rabah khenata, A. B., M. Sahnounb, Ali. H. Reshakd, H. Baltacheb, M. Rabaha. (2006). Elastic, electronic and optical properties of ZnS, ZnSe and ZnTe under pressure. *Computational Materials Science*, 38(1), 29-38.
- S. Ves, U. S., N. E. Christensen, K. Syassen, and M. Cardona. (1990). Cubic ZnS under pressure: Optical-absorption edge, phase transition, and calculated equation of state. *PHYSICAL REVIEW B*, 42(14).

- S.Q. Wang. (2006). First-principle study of the anisotropic thermal expansion of Wurtzite ZnS. *Applied Physics Letters*, 88(6).
- Shimono, Y. I. W. (2003). Comparison of electronic structures of doped ZnS and ZnO calculate by a first-principle pseudopotential method. *Journal of Materials Science: Materials in Electronics*, 14(3), 149-156.
- Singh, J. (2005). *Smart Electronic Materials: Fundamentals and Applications*. United Kingdom: Cambridge university press.
- Wang, J. P. P. a. Y. (1992). Accurate and simple analytic representation of the electron-gas correlation energy. *PHYSICAL REVIEW B*, 45(23).